Carbon and group II acceptor coimplantation in GaAs

R. Morton[a] and S. S. Lau
Electrical Computer Engineering Department, University of California, San Diego, La Jolla, California 92093-0407

D. B. Poker
Oak Ridge National Laboratory, Oak Ridge, Tennessee 37831

P. K. Chu
Department of Physics and Materials Science, City University of Hong Kong, Hong Kong

K. K. Fung
Department of Physics, The Hong Kong University of Science and Technology, Hong Kong

N. Wang
Department of Physics and Materials Science, City University of Hong Kong, Hong Kong

(Received 27 February 1998; accepted for publication 17 July 1998)

Coimplantations of carbon and one of the group II acceptors, Mg, Zn, or Cd, were performed and compared to implantations involving only a single element (Mg, Zn, or Cd) or Ga and C coimplanted into GaAs substrates. The group II and C (II/C) coimplantations act to balance the crystal stoichiometry since group II atoms prefer to reside in the Ga sublattice and C prefers to reside in the As sublattice. The electrical characteristics of the various implantations were obtained from sheet and differential Hall measurements. Rutherford backscattering spectrometry was employed to determine the amount of implantation-induced damage which was then correlated to the amount of C activation in the group II/C coimplanted samples. It was found that coimplantation of the heavier group II acceptors, Zn and Cd, resulted in layers with larger peak hole concentrations. This is a result of the large amount of lattice damage created by these elements which is thought to provide the necessary abundance of As vacancies for C activation. Secondary ion mass spectroscopy measurements of the samples after implant activation indicate that C coimplantation significantly reduces the diffusivity of the group II acceptors. Cross-sectional transmission electron microscopy indicated a unique defect structure (extrinsic dislocation loops) for the cases of group II/C coimplantation. These dislocation loops are located at the diffusion front of the group II element in the samples and therefore have a rather profound influence on the diffusion of the group II elements. A rationalization of the defect structure and the effect it has on the diffusion of group II elements is given. © *1998 American Institute of Physics.* [S0021-8979(98)07220-X]

I. INTRODUCTION

Ion implantation technology for *p*-type doping in GaAs needs to satisfy two essential criteria for the realization of high performance electronic devices: reproducible electrical and spatial control of the dopant species. Implanted layers that satisfy these requirements have received recent attention for use in the fabrication of junction field effect devices because of their increased gate turn on voltage and the resulting reduced gate leakage compared to conventional metal-semiconductor field-effect transistor devices.[1] With the recent demonstration of a *p*-channel GaAs based metal-oxide-semiconductor field-effect transistor,[2] ion implantation techniques for highly doped *p*-type source and drain regions may become more important.

The use of coimplantation to maintain stoichiometry in compound semiconductors was first proposed by Heckingbottom and Ambridge.[3] They theorized that the use of carefully matched dual implants in GaAs could avoid many of the complications which arise from disturbing the stoichiometry when a single species is introduced into a compound semiconductor. Over the years this theory has been validated by a number of researchers for both *n*-type and *p*-type GaAs. In addition, there are complications which arise from radiation damage related phenomenon in compound semiconductors which can dominate doping studies.[4]

Coimplantation of group V elements with group II acceptors has produced layers with enhanced electrical activation as well as limited group II redistribution after annealing. These studies have utilized the following coimplantation schemes: Mg/As,[5–7] Mg/P,[8] Zn/As,[9,10] and Zn/P.[11] Many of these studies speculated that the diffusion of the group II element is reduced when coimplantation is employed because of an increased substitutionality of the group II element on the Ga sublattice. Once incorporated onto the Ga sublattice the rapid diffusion of the group II element is reduced due to the disappearance of the fast diffusing group II interstitials (II_I).

Carbon, a group IV element which becomes a *p*-type acceptor on the As sublattice, has received much attention

[a]Electronic mail: rickm@tqs.com

 © 1998 American Institute of Physics

because of its low diffusion coefficient in GaAs when compared to the group II acceptors.[12] In general, the diffusion coefficients of the group II acceptors are proportional to the square of the group II concentration, or hole concentration.[13–16] Their rapid diffusivity at high carrier concentration limits their use in applications where shallow or abrupt junctions are required. Implanted C is unique as an acceptor in GaAs in that radiation damage is necessary in order to achieve considerable electrical activation.[17–21] The radiation damage provides As vacancies that become sites for carbon activation.[21] Carbon, because of its relatively light mass, is not effective in creating implantation damage in GaAs, and therefore poor activation results when implanted alone. Implantation with heavier elements increases activation, but consideration must also be made concerning the chemical nature of the coimplant. Group III coimplantation species, which tend to increase the As-related vacancies, provide superior electrical activation of the implanted C.[21] These coimplantation schemes attempt to balance the III–V stoichiometry by providing an element that prefers the group III sublattice and consequently assists the incorporation of C onto the As sublattice. The present study utilizes heavy group II elements such as Zn and Cd to create damage so that the C atoms can reside on As sites preferentially. The group II elements can also serve as acceptors by residing on the Ga sites.

II. EXPERIMENT

The substrates used for this study were epiready semi-insulating vertical gradient freeze (100) GaAs. All implantations were performed 7° off the ⟨100⟩ axis, with the C implantation preceding group II or Ga implantation. The coimplantation energies were chosen using TRIM simulation to calculate the ion profiles. In order to overlay the ion profile of the 45 keV C implantation the energies of the Mg, Zn, Cd, and Ga ions were 80, 215, 370 and 230 keV, respectively. Implantation doses of $5\times10^{14}\ cm^{-2}$ and $1\times10^{15}\ cm^{-2}$ were used to make different comparisons between the electrical and the redistribution characteristics of the various implantation schemes studied.

Activation annealing was performed in a rapid thermal annealer employing the proximity method with a flowing forming gas ambient ($85\%N_2/15\%H_2$). For electrical characterization van der Pauw geometry Hall measurements were made using In(Zn) contacts. Differential Hall effect measurements were made by etching the implanted layer sequentially using a dilute solution of H_2SO_4:30%H_2O_2:H_2O in a 1:1:100 ratio by volume. The etch rate was calibrated using Dektak stylus profilometry to be approximately 60 Å/min. Rutherford backscattering spectrometry (RBS) and channeling techniques using a 2.3 MeV He^{++} beam were employed to measure the amount of implantation induced damage. A scattering angle of 170° was used, and the channeling measurements were performed along the ⟨100⟩. The thicknesses of the amorphous layers created by the heavier ions used in this study were estimated by measurement of the energy width of the signal taken from the amorphous layer as specified in Ref. 22. Secondary ion mass spectroscopy (SIMS) measurements using a Cameca IMS-4*f* microanalyzer were performed to compare the redistribution of the group II elements with and without the carbon coimplantation. A Cs ion beam at an impact energy of 14.5 keV was used. The group II-Cs^+ molecular species ($MgCs^+$, $ZnCs^+$, $CdCs^+$) were analyzed, which gives good detection limits for Mg, Zn, and Cd. The SIMS concentration profiles obtained are within 15% accuracy in concentration and 10% accuracy in the depth scale. The microstructures of the different samples were examined by cross-sectional transmission electron microscopy (XTEM) and high resolution electron microscopy (HREM).

TABLE I. Sheet hole concentrations as determined from Hall measurements for the various implantation schemes studied.

Implanted species	Implanted dose (cm^{-2})	Sheet hole concentration ($10^{14}\ cm^{-2}$)
C-only	5×10^{14}	0.07
Ga/C	$5\times10^{14}/5\times10^{14}$	2.1
Ga/C	$1\times10^{15}/1\times10^{15}$	2.5
Zn-only	5×10^{14}	2.9
Zn-only	1×10^{15}	5.2
Zn/C	$5\times10^{14}/5\times10^{14}$	4.4
Cd-only	5×10^{14}	2.6
Cd-only	1×10^{15}	5.2
Cd/C	$5\times10^{14}/5\times10^{14}$	4.8
Mg-only	5×10^{14}	1.4
Mg-only	1×10^{15}	1.9
Mg/C	$5\times10^{14}/5\times10^{14}$	1.1

III. RESULTS AND DISCUSSION

A. Electrical results: Correlation with implantation induced damage

Table I summarizes the sheet carrier concentrations obtained for the implantation schemes investigated. These results were obtained at optimum annealing temperatures, reported in an earlier work, which was 820 °C for the samples containing any of the group II species, and 900 °C for the Ga/C coimplantations and C-only implantations.[23] The implanted doses for the samples are listed in Table I. As shown in the table, C implanted alone shows poor activation due to the lack of any significant lattice damage. Carbon implantation alone did not create any significant lattice damage as measured by RBS (not shown). The Ga coimplantation increases C activation significantly by increasing the measured sheet hole concentration from $7\times10^{12}\ cm^{-2}$ to $2.1\times10^{14}\ cm^{-2}$. The RBS spectra in Fig. 1(a) indicates that the Ga coimplantation created an amorphous layer approximately 1500 Å thick. As previously mentioned, this damage is necessary for a more efficient activation of implanted carbon. However, only a small increase in the sheet hole concentration is seen when the dose is increased from $5\times10^{14}\ cm^{-2}$ to $1\times10^{15}\ cm^{-2}$ (see Table I). This is a result of the peak hole concentration saturating near $1\times10^{19}\ cm^{-3}$ in these samples, so a further increase in dose results in only a slightly broader hole profile. Earlier studies on carbon-implanted GaAs reported that the maximum con-

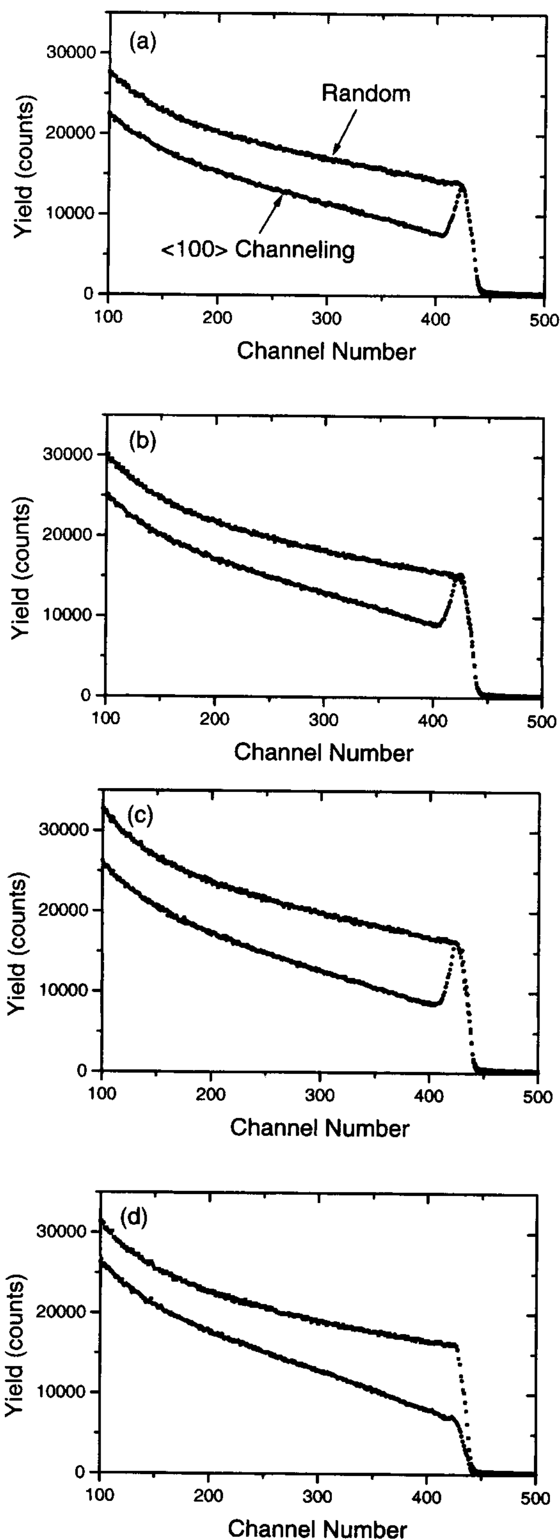

FIG. 1. Random and ⟨100⟩ channeling spectra for as-implanted samples: (a) Ga/C coimplantation (5×10^{14} cm^{-2}/5×10^{14} cm^{-2}), (b) Zn/C coimplantation (5×10^{14} cm^{-2}/5×10^{14} cm^{-2}), (c) Cd/C coimplantation (5×10^{14} cm^{-2}/5×10^{14} cm^{-2}), and (d) Mg/C coimplantation (5×10^{14} cm^{-2}/5×10^{14} cm^{-2}). The incident He^{++} energy was 2.3 MeV and the detector angle was set at 170°.

centration of free carriers does not exceed values in the low 10^{19} cm^{-3}. Carbon precipitation and the formation of dicarbon centers are both possible mechanisms for this observed saturation in the free hole concentration.[24,25] In the case of

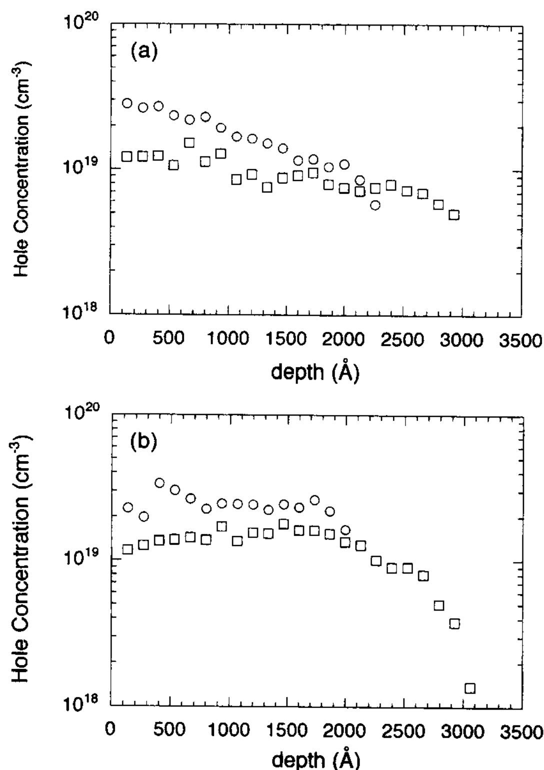

FIG. 2. Carrier profiles determined from differential Hall measurements for: (a) Zn-only (□) (1×10^{15} cm^{-2}) and Zn/C (○) coimplantation (5×10^{14} cm^{-2}/5×10^{14} cm^{-2}), and (b) Cd-only (□) (1×10^{15} cm^{-2}) and Cd/C (○) coimplantation (5×10^{14} cm^{-2}/5×10^{14} cm^{-2}).

II/C coimplantations, the Zn/C coimplantation (5×10^{14} cm^{-2}/5×10^{14} cm^{-2}) gives a higher sheet carrier concentration than the sum of the C-only and the Zn-only implantations (5×10^{14} cm^{-2}) at a combined dose of 1×10^{15} cm^{-2}, as shown in Table I. Figure 1(b) shows that an amorphous layer similar to that created by Ga coimplantation (~1500 Å in thickness) is formed by the Zn/C coimplantation. This coimplantation enhances the acceptor contribution from C atoms. Cadmium, the heaviest of the coimplant ions used in this study, forms an amorphous layer approximately 1800 Å thick, as shown in Fig. 1(c). This results in a similar enhancement of the activation of the implant C as shown in Table I. Samples with Mg implantations result in the lowest activation of all the group II elements studied. Furthermore, samples implanted with both C and Mg have a lower sheet carrier concentration than those implanted with Mg only. This is due to the redistribution properties of the Mg upon activation which will be discussed in Sec. III B. Magnesium, the lightest of the coimplantation species studied, failed to create a heavily damaged layer needed for C activation, as shown in the RBS spectra in Fig. 1(d) for the Mg/C coimplantation. These results offer solid evidence of the importance of implantation damage for the activation of implanted carbon.

The carrier profiles for the Zn-only (1×10^{15} cm^{-2}) and the Zn/C (5×10^{14} cm^{-2} each) coimplantation are given in Fig. 2(a), and for the Cd-only and Cd/C cases in Fig. 2(b). Note that for the group II/C cases, (represented by empty circles in the figure) there is a higher peak hole concentration

($\sim 3\times 10^{19}$ cm^{-3}) near the surface and the profile remains much closer to the surface. The group II-only implants (depicted by empty squares) have redistributed to yield a lower maximum carrier concentration of approximately 1×10^{19} cm^{-3}, with a more extended dopant profile.

We note from Table I that the sheet carrier concentration for Zn-only implantation (1×10^{15} cm^{-2}) is higher than that for Zn/C coimplantation (5×10^{14} cm^{-2} each). The same is also true for the Cd-only and the Cd/C coimplantation. From the results shown in Figs. 2(a) and 2(b) it is apparent that the higher sheet concentration for group II-only implantation is due to a much more diffused dopant profile. The group II/C coimplantations give a higher hole concentration in volume density near the surface and provide a much shallower junction. Our results of the Zn/C and the Cd/C coimplantation indicate that both the group II and the carbon atoms contribute to the hole concentration.

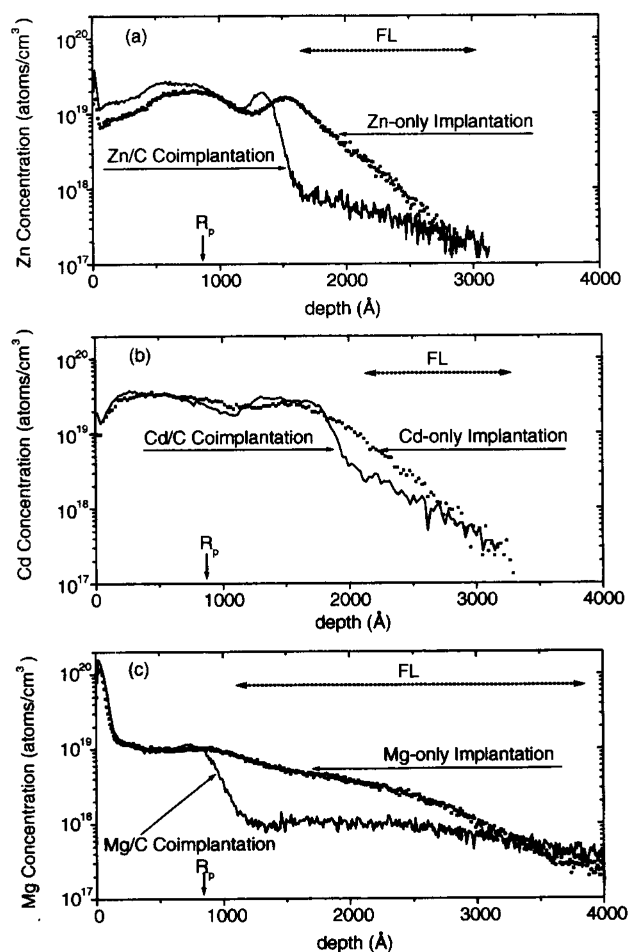

FIG. 3. Group II SIMS profiles for annealed samples comparing the distributions of group II only implantation (5×10^{14} cm^{-2}) to those obtained when group II/C coimplantation (5×10^{14} cm^{-2}/5×10^{14} cm^{-2}) is used. (a) Zn SIMS profiles for Zn-only implantation (dotted line) and Zn/C coimplantation (solid line). (b) Cd SIMS profiles for Cd-only implantation (dotted line) and Cd/C coimplantation (solid line). (c) Mg SIMS profiles for Mg-only implantation (dotted line) and Mg/C coimplantation (solid line). The areas marked FL are depths where a network of Frank loops were observed by TEM in the C-coimplanted samples (Sec. III C). The projected range, R_p, of the as-implanted group II species is shown in the figures for reference.

B. Group II redistribution

The group II profiles for the single implants and the group II/C coimplants have been investigated using SIMS measurements. The results are shown in Fig. 3. A double hump profile was observed in samples containing Zn and Cd implantations. A "kink-and-tail" profile was observed in all of the coimplanted samples shown in the figure.

Studies involving group II dopants have shown that at high concentrations the diffusivities of these impurities are strongly influenced by the group II acceptor and other defect concentrations.[26] This can be understood in terms of the interstitial-substitutional mechanism by which the group II impurities are thought to diffuse. One of the widely accepted diffusion theories is the "kick-out" mechanism.[26,27] In this model a Ga interstitial (I_{Ga}) is created when a diffusing group II interstitial (II_I) displaces a Ga atom from its sublattice. Gosele[26] and Tan[27] have shown the reaction to be:

$$\mathrm{II}_I^+ \Leftrightarrow II_{\mathrm{Ga}}^- + I_{\mathrm{Ga}}^0 + 2h^+, \tag{1}$$

where II_{Ga} is a substitutional group II acceptor atom on the Ga sublattice. It should be noted that the charge state of the species in (1) have been assigned to various values reported in the literature.[28] However, we will use this equation for the general basis of our discussion. Using this model and the law of mass action the following dependence for the effective diffusivity of the group II acceptor (D_{eff}) can be obtained:[29]

$$D_{\mathrm{eff}} \propto [I_{\mathrm{Ga}}]\times p^2, \tag{2}$$

where p is the hole concentration. Group II diffusion is enhanced by the concentration of Ga interstitials and the square of the hole concentration. In simple physical terms, the concentration of the fast diffusing group II interstitials is increased by the presence of Ga interstitials which compete for the Ga sublattice sites. As a result the diffusion of group II elements is enhanced in a Ga-rich region in the sample.[30] A Ga-rich region can be formed in the implanted samples in two ways: (1) the kick-out mechanism provides a supersaturation of Ga interstitials at the diffusion front,[26,27] (2) the recoil nature of the implantation process creates an excess of Ga matrix atoms located at greater depths due to a slight mass differential between Ga and As.[31]

For the As sublattice, the presence of the implanted C atoms increases the As interstitial concentration due to the competition between C and As for the As sublattice sites. This has the effect of creating a localized As-rich region in the sample. In this respect the presence of implanted C is similar to that of annealing GaAs samples in an As overpressure, where the As vacancy and the Ga interstitial concentrations are reduced as dictated by the mass action relationship:

$$[I_{\mathrm{Ga}}] \quad \text{and} \quad [V_{\mathrm{As}}] \propto P_{\mathrm{As}_4}^{-1/4}, \tag{3}$$

where P_{As_4} is the As_4 vapor pressure.[27] As a result of the reduced Ga interstitial concentration the diffusion of the group II elements is also reduced in the As-rich region [see Eq. (2)]. Carbon is known to be relatively immobile, therefore the electrically active group II and C (occupying substi-

tutional sites) concentrations are higher in this region. This can be prominently seen in the SIMS profile shown in Fig. 3(a) for the Zn/C sample (solid line) where a higher concentration of Zn is located in the first 1000 Å. At greater depths, in the region where the Ga recoil distribution exists, the gallium interstitials have a higher concentration. This leads to a faster diffusion rate of the group II elements, which reduces the group II concentration in this region, as demonstrated by the dip in the profile, approximately 1200 Å from the surface, shown in Fig. 3(a). The formation of the double hump profiles also observed in the Zn-only, Cd-only, and Cd/C implantations is due to this same mechanism. At even greater depths in the C and group II coimplanted cases the diffusing I_{Ga} and I_{As} recombine to form extrinsic dislocation loops, thus greatly reducing both interstitial species. These loops serve as sinks for both interstitial species thus significantly reducing the diffusion of the group II elements. The dislocation loops, known as Frank loops (FL) because of their extrinsic nature, are located just beyond the high concentration region of the profile (as indicated in the figures). The defect structure will be discussed in the following section.

The absence of the double hump profile in the Mg cases is due to less radiation damage and a smaller Ga recoil distribution because of the light masses of Mg and C. The severe outdiffusion present in samples implanted with Mg explains their reduced conductivity seen in Sec. III A [see Fig. 3(c)]. Also the Mg/C sample exhibited a lower sheet carrier concentration than that of the Mg-only implant because the indiffusion is limited, but rapid outdiffusion takes place; both of these effects reduce the total number of carriers. In all the cases studied the surface of the sample acts as an efficient sink for point defects, therefore, the surface effect dominates the distribution of various species near the surface, rather than the fore-mentioned diffusion mechanism in the bulk.

C. Microstructure evaluation

Cross-sectional TEM, XTEM, was used to investigate the defect structures in the samples shown in Fig. 4. Present in all samples (group II-only and C coimplanted) were fairly large dislocation loops with intrinsic or extrinsic faults inside, labeled DL in Fig. 4. These defects are commonly observed in implanted GaAs. These large loops are seen to form on the {111} and {110} planes. Significant difference in microstructure has been observed towards the tail of the group II diffusion profiles between group II only and group II/C coimplants. Samples that have been coimplanted with C all contain a network of Frank loops, labeled FL in Figs. 4(a), 4(c), 4(e), and 4(g). The location of these loops is in the tail region of the diffusion profile, as indicated in the SIMS results shown in Fig. 3. The micrographs of the group II only implanted samples are shown next to the carbon coimplanted samples so that the absence of the dense network of dislocation loops is readily apparent. The HREM image in Fig. 4(h) confirms the extrinsic nature of the dislocation loops present in the carbon coimplanted samples. This particular lattice image shows a dislocation loop aligned with the {111} plane. Most of the loops are along the {111} planes, but a small number of loops were found to have formed along the {100} planes. These dislocation loops are the result of the condensation of point defects and act as sinks to restore the point defects to their dynamical equilibrium condition. By maintaining the point defect concentrations at their dynamical equilibrium values these dislocation loops limit the indiffusion of the group II elements. The same dislocation loops are seen in the case of Ga/C coimplantation in Fig. 4(g). Here the excess Ga interstitials are introduced by both the implantation of Ga and its associated damage. The fact that a dense network of Frank loops is seen only in the cases of C coimplantation provides evidence that the excess As that is generated by C incorporation is key to the dislocation loop formation. These dislocation loops reside much deeper in the Ga/C sample than the other cases studied probably due to the higher anneal temperature used for these samples, which was 900 °C as opposed to 820 °C for other samples.

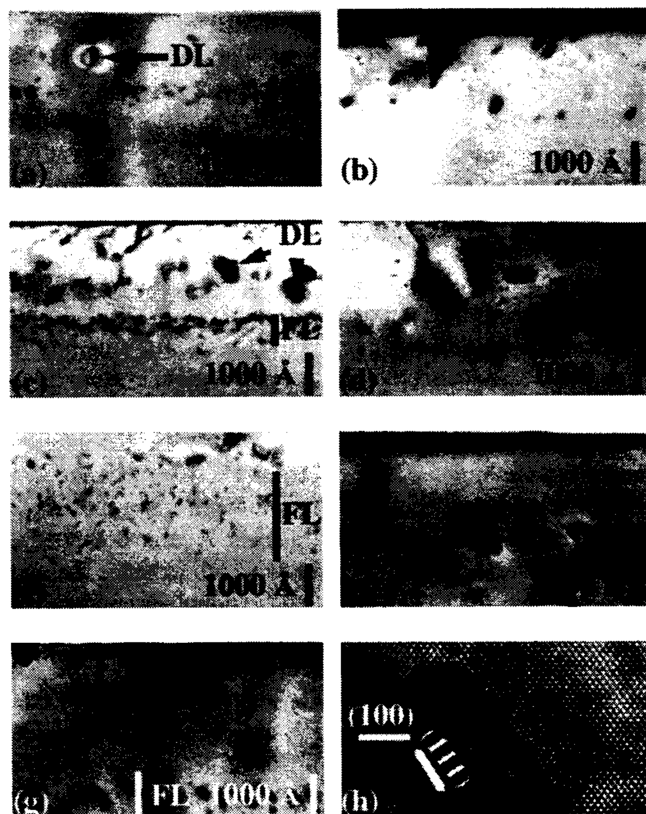

FIG. 4. XTEM micrographs for samples after implantation activation. (a) Zn/C coimplanted sample (5×10^{14} cm^{-2}/5×10^{14} cm^{-2}), (b) Zn-only implanted sample (5×10^{14} cm^{-2}), (c) Cd/C coimplanted sample (5×10^{14} cm^{-2}/5×10^{14} cm^{-2}), (d) Cd-only implanted sample (5×10^{14} cm^{-2}), (e) Mg/C coimplanted sample (5×10^{14} cm^{-2}/5×10^{14} cm^{-2}), (f) Mg-only implanted sample (5×10^{14} cm^{-2}), (g) Ga/C coimplanted sample (5×10^{14} cm^{-2}/5×10^{14} cm^{-2}). Examples of the large dislocation loops seen in all the samples are labeled DL in Figs. 4(a) and 4(c). The dense network of Frank loops are labeled FL in the C-coimplanted samples. (h) Lattice image revealing the extrinsic nature of the dislocation loops formed in the samples coimplanted with C. A majority of the loops were found to be orientated along the {111} plane. This particular loop was present in the Ga/C coimplanted sample.

IV. SUMMARY

In this investigation we found that the coimplantation of C with Zn and Cd in GaAs provides the necessary lattice

damage needed for C activation. These two implantation schemes (Zn/C and Cd/C) provide a way of raising the peak hole concentration by supplying acceptors on both the Ga and As sublattices. On the other hand, Mg/C coimplantation fails to create the lattice damage required for C activation. The coimplantation of C with group II elements creates an As-rich layer, compared to samples where only group II elements were implanted. This As-rich region has the effect of limiting the group II redistribution in this region, as a result, a kink-and-tail profile is observed similar to that for Zn in-diffusion experiments with an As over pressure. This profile is the direct consequence of the As-rich region, created by C coimplantation, and the Ga-rich region, created by the diffusing group II species. For the cases of Zn and Cd implantation a double-hump diffusion profile is observed, independent of C coimplantation. This characteristic is a result of the lattice damage created by these elements. A large component of this damage is the Ga interstitials which enhance Zn and Cd diffusion in the saddle point of the double-hump profile. A network of Frank loops was observed in all samples coimplanted with C. These loops are thought to result from the condensation of point defects, Ga and As interstitials, that exist in that region. In doing so, the concentration of Ga interstitials is decreased at the diffusion front compared to cases where the dislocation loops do not form (group II only implantations). Due to the reduction of Ga interstitials the diffusion of the group II element is reduced in the region where the Frank loops are present.

ACKNOWLEDGMENTS

UCSD acknowledges the financial support of the National Science Foundation. R.M. acknowledges the AASERT Graduate Study Program from ARPA via ONR. The work of ORNL was sponsored by the Division of Materials Science, U. S. Department of Energy, under Contract No. DE-AC05-96OR22464 with Lockheed Martin Energy Research Corporation. The work done at HKUST acknowledges the Matching Funds Grant MFG94/95.SC.022.

[1] J. C. Zolper, A. G. Baca, R. J. Shul, A. J. Howard, D. J. Rieger, M. E. Sherwin, M. L. Lovejoy, H. P. Hjalmarson, B. L. Draper, J. F. Klem, and V. M. Hietala, IEEE Trans. Electron Devices **41**, 1078 (1994).
[2] F. Ren, M. W. Hong, W. S. Hobson, J. M. Kuo, J. R. Lothian, J. P. Mannaerts, J. Kwo, Y. K. Chen, and A. Y. Cho, Tech. Dig. Int. Electron Devices Meet., 10.7.1 (1996).
[3] R. Heckingbottom and T. Ambridge, Radiat. Eff. **17**, 31 (1973).
[4] T. E. Haynes, R. Morton, and S. S. Lau, Appl. Phys. Lett. **64**, 991 (1994).
[5] K. K. Patel and B. J. Sealy, Appl. Phys. Lett. **48**, 1467 (1986).
[6] A. N. M. Masum Choudhury and C. A. Armiento, Appl. Phys. Lett. **50**, 448 (1987).
[7] G. Landgren and W. H. van Berlo, J. Appl. Phys. **63**, 2783 (1988).
[8] K. Morizuka, T. Nozu, and M. Azuma, Electron. Lett. **22**, 315 (1986).
[9] J. Kasahara, K. Taira, Y. Kato, M. Arai, and N. Watanabe, Jpn. J. Appl. Phys., Part 2 **22**, L373 (1983).
[10] D. E. Davies and P. J. McNally, Appl. Phys. Lett. **44**, 304 (1984).
[11] A. C. T. Tang, B. J. Sealy, and A. Rezazadeh, Electron. Lett. **25**, 861 (1989).
[12] T. J. de Lyon, J. M. Woodall, M. S. Goorsky, and P. D. Kirchner, Appl. Phys. Lett. **56**, 1040 (1990).
[13] W. V. McLevige, K. V. Vaidyanathan, and B. G. Streetman, Appl. Phys. Lett. **33**, 127 (1978).
[14] P. Enquist, G. W. Wicks, L. F. Eastman, and C. Hitzman, J. Appl. Phys. **58**, 4130 (1985).
[15] M. A. H. Kadhim and B. Tuck, J. Mater. Sci. **7**, 68 (1988).
[16] Although in some cases Be diffusion is directly proportional to the concentration of holes. For an example see: H. G. Robinsoń, M. D. Deal, and D. A. Stevenson, Appl. Phys. Lett. **58**, 2800 (1991).
[17] B. K. Shin, J. E. Ehret, Y. S. Park, and M. Stefiniw, J. Appl. Phys. **49**, 2988 (1978).
[18] S. J. Pearton and C. R. Abernathy, Appl. Phys. Lett. **55**, 678 (1989).
[19] W. H. van Berlo, J. Appl. Phys. **73**, 2765 (1993).
[20] S. T. Horng and M. S. Goorsky, Appl. Phys. Lett. **68**, 1537 (1996).
[21] A. J. Moll, K. Man Yu, W. Walukiewicz, W. L. Hansen, and E. E. Haller, Appl. Phys. Lett. **60**, 2383 (1992).
[22] W. K. Chu, J. W. Mayer, and M.-A. Nicolet, *Backscattering Spectrometry* (Academic, New York, 1978), p. 247.
[23] R. Morton, S. S. Lau, D. B. Poker, and P. K. Chu, Appl. Phys. Lett. **68**, 1135 (1996).
[24] A. J. Moll, E. E. Haller, J. W. Ager III, and W. Walukiewicz, Appl. Phys. Lett. **65**, 1145 (1994).
[25] J. Wagner, R. C. Newman, B. R. Davidson, S. P. Westwater, T. J. Bullough, T. B. Joyce, C. D. Latham, R. Jones, and S. Öberg, Phys. Rev. Lett. **78**, 74 (1997).
[26] U. Gösele and F. Morehead, J. Appl. Phys. **52**, 4617 (1981).
[27] T. Y. Tan, U. Gösele, and S. Yu, Crit. Rev. Solid State Mater. Sci. **17**, 47 (1991).
[28] R. M. Cohen, J. Appl. Phys. **67**, 7268 (1990).
[29] H. G. Robinson, M. D. Deal, and D. A. Stevenson, Appl. Phys. Lett. **56**, 554 (1990).
[30] W. Jäger, A. Rucki, K. Urban, H. G. Hettwer, N. A. Stolwijk, H. Mehrer, and T. Y. Tan, J. Appl. Phys. **74**, 4409 (1993).
[31] L. A. Christel and J. F. Gibbons, J. Appl. Phys. **52**, 5050 (1981).